TRR
JOURNAL OF THE TRANSPORTATION RESEARCH BOARD

Article

Transportation Research Record
1–13

DOI: 10.1177/0361198118758631
journals.sagepub.com/home/trr
SAGE

Soil–Geosynthetic Interface Shear in Different Testing Scales

Gholam H. Roodi[1], Amr M. Morsy[1], and Jorge. G. Zornberg[1]

Abstract

Geosynthetics have been used to improve mechanical performance of roadway layers (e.g., geosynthetic-reinforced asphalt, geosynthetic-stabilized bases) and a wide range of transportation infrastructures (e.g., geosynthetic-reinforced soil walls). A key aspect in understanding soil–geosynthetic interaction mechanisms involved in each application includes characterization of the interface between geosynthetics and adjacent materials. This study evaluates soil–geosynthetic interface shear in various pullout test scales including standard, smaller than standard, and larger than standard scales. Experimental results obtained from tests conducted in each scale were analyzed to determine the soil–geosynthetic interface shear model. An iteration procedure, similar to that used in *t*–*z* analysis of pile loading, was developed to simulate incremental geosynthetic movements. Shape and parameters of the interface shear model were changed to minimize the residual error between experimental and simulated data. It was found that mobilization of the interface shear in the small-scale test differs from that in the standard- and large-scale tests. In the standard- and large-scale tests, the ultimate soil–geosynthetic interface shear mobilized at comparatively small displacements, which could be represented by a linear plastic interface shear model. In the small-scale test, however, the interface shear developed in two phases. A portion of the ultimate interface shear mobilized at comparatively small displacements while additional resistance continued to mobilize at extended displacements. Consequently, the development of interface shear resistance in the standard- and large-scale tests was found to depend on progressive increase of the geosynthetic mobilized length, whereas in the small-scale test the interface shear resistance developed by displacement of the entire geosynthetic.

Geosynthetics have been widely used to improve mechanical performance of pavement layers as well as a wide range of transportation infrastructures. Specifically, geosynthetic layers have been used to reinforce hot mix asphalt concrete (*1*), to stabilize unbound granular base course (*2,3*), to stabilize subgrade layer, and to reinforce backfill materials in retaining structures (*4,5*). Quantification of the benefits derived from the use of geosynthetics in each application requires understanding characteristics of the geosynthetic material, the surrounding materials, and the soil–geosynthetic interaction.

Soil–geosynthetic interaction has typically been evaluated using interface direct shear and pullout tests (*6,7*), which mobilize the soil–geosynthetic interface shear in different modes. Pullout test would be relevant in cases where elongation of the geosynthetic specimen is considered. Results obtained from pullout tests have been used to gain better understanding of (1) ultimate conditions in structures that are designed using limit states conditions (e.g., geosynthetic-reinforced soil walls) (*4,8*) and (2) service conditions in structures that are designed using serviceability criteria (e.g., geosynthetic-stabilized roadways) (*9,10*).

This study evaluates soil–geosynthetic interface shear in three pullout test scales including: a standard scale, a significantly smaller and a larger than standard scales. Experimental results obtained from tests conducted in the three scales were analyzed to estimate soil–geosynthetic interface shear model that governed the response in each scale. An iteration procedure, similar to that used in *t*–*z* analysis of pile loading, was developed to simulate incremental geosynthetic movements. The soil–geosynthetic interface shear model was optimized to minimize the residual error between experimental and simulated data.

Background

Modeling soil–geosynthetic interaction requires suitable constitutive relationships to be defined for the soil, the geosynthetic, and the soil–geosynthetic interface. Although the unit tension–strain response of geosynthetics is inherently

[1]Department of Civil, Architectural, and Environmental Engineering, The University of Texas at Austin, Austin, TX

Corresponding Author:
Address correspondence to Gholam H. Roodi: hroodi@utexas.edu

nonlinear, a linear response has often been adopted (*11–13*). Nonlinear functions have also been used, including polynomial functions (*14,15*) and hyperbolic functions (*16*).

Interface constitutive relationships relate the shear stress mobilized at the soil–geosynthetic interface to the relative displacements that are mobilized between the two materials. Models adopted in previous studies to describe the interface interaction include: linear elastic (*13*); linear elastic–perfectly plastic (*11,14*); rigid–perfectly plastic (*12*); bilinear and hyperbolic models (*15*); and more complex nonlinear multiphase models such as elasto-plastic strain hardening and softening models (*11,16*).

This study focuses on determining the soil–geosynthetic interface shear model in various scales of pullout testing. Unlike conventional approaches in evaluation of pullout test results, in which constitutive models for soil–geosynthetic interface shear and geosynthetic material were typically determined using additional tests (e.g., direct shear test, wide width tensile test), this study adopted a procedure in which the pullout test results can directly be used to identify constitutive models for the geosynthetic and the soil–geosynthetic interface shear.

Factors that may affect the pullout test results include thickness of the soil, dimensions of the geosynthetic specimen, loading rate, and friction between soil and the side and front walls of pullout box (*17–19*). The large volume of soil and extensive efforts required to conduct experiments in large scales makes the use of this scale particularly onerous in studies where production of large volume of data is essential. In addition, although avoiding boundary effects may be essential in studies on large-displacement parameters, when the focus is on ultimate condition, studies on stiffness parameters, when the focus is on the response under small displacements, may not be sensitive to boundary effects. The results obtained in this study underscore that the difference between the pullout test data in various testing scales may partially be attributed to the different soil–geosynthetic interface shear models that govern the response in each scale.

Methodology

Pullout tests were conducted and results were back-analyzed to predict the constitutive models for geosynthetic and soil–geosynthetic interface. The constitutive model for the geosynthetic was obtained using data collected from the unconfined length of the geosynthetic. The constitutive model for soil–geosynthetic interface was estimated by simulation of the pullout data in the confined length using a procedure similar to *t–z* analysis procedure originally developed for simulation of deep foundations subjected to axial loading (*20*). This procedure and specific algorithm to simulate pullout test data are presented next.

t–z *Analysis*

The *t–z* analysis approach is a method that was developed to predict the load transfer between piles and surrounding soils. This method is deemed as one of the most widely used techniques to estimate the settlement of individual axially loaded piles. This approach involves modeling the pile as a series of discrete elements connected axially by nonlinear springs, which represent the axial stiffness of the pile. In addition, these elements are connected through their skin to surrounding soil by other nonlinear springs (*t–z* relationship), which represent the resistance of the soil in skin friction. An additional nonlinear spring is assumed at the pile tip, which represents the end-bearing (*q–y* relationship). Several research studies were conducted and obtained *t–z* and *q–y* relationships empirically based on model and full-scale pile load tests (*21*). Subsequent studies proposed general recommendations for estimating *t–z* and *q–y* curves (*22*). Theoretical approaches have also been developed to relate the *t–z* and *q–y* relationships to the soil properties surrounding the pile (*23,24*). A few studies have also adopted *t–z* analysis to simulate geosynthetic pullout test results (*11*, *25*, *26*).

Solution Algorithm for Pullout Test Data

The general approach adopted in this study to simulate experimental pullout test data involves discretizing the geosynthetic specimen into several segments, adopting an incremental displacement to the free end of the geosynthetic, and satisfying the force equilibrium equation of each segment using an iterative procedure to eventually determine the displacement, strain, interface shear, and load profile along the geosynthetic length. The constitutive model for soil–geosynthetic interface was used to estimate the interface shear resistance mobilized along each segment. This model relates geosynthetic displacement (u) to the interface shear between soil and the geosynthetic (τ):

$$\tau = f(u) \tag{1}$$

The model adopted for geosynthetic material was used to estimate the unit tension developed in the geosynthetic. This model relates geosynthetic unit tension (T) to its tensile strain (ε):

$$T = g(\varepsilon) \tag{2}$$

Specific steps adopted in this study to implement the *t–z* analysis procedure to simulate pullout test data are as follows:

Step 1: The geosynthetic specimen is discretized into several segments from 1 (at the loading front) to n (at the free end). Definitions used in discretization of the geosynthetic specimen are presented in Figure 1. Geosynthetic nodal displacements, unit tension in the geosynthetic at the nodal locations, interface shear between soil and geosynthetic segments, and tensile strain in the geosynthetic are defined by u, T, τ, and ε, respectively.
Step 2: An incremental displacement, δu, is adopted at the free end of the geosynthetic (Segment n):

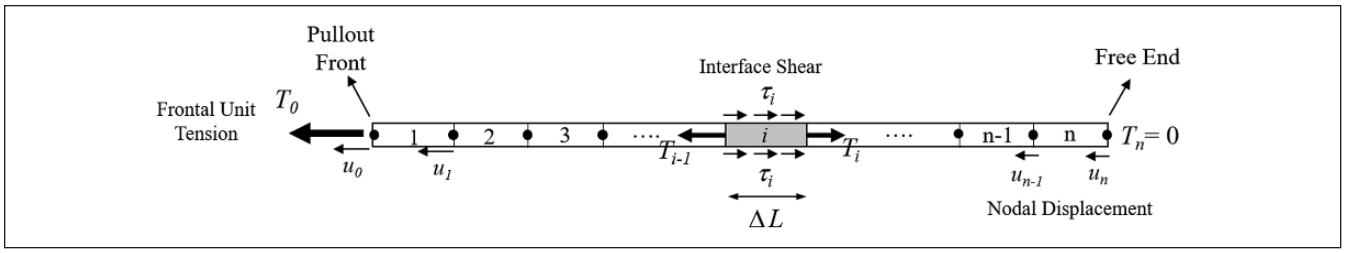

Figure 1. Discretization of geosynthetic along with definition of variables.

$$u_n = \delta u \tag{3}$$

The unit tension at the free end of geosynthetic is zero:

$$T_n = 0 \tag{4}$$

Step 3: Displacement at the front of Segment *n* is assumed (u_{n-1}) and the average displacement in Segment *n* ($u_{n(avg)}$) is estimated as follows:

$$u_{n(avg)} = \frac{u_n + u_{n-1}}{2} \tag{5}$$

Step 4: The interface shear along Segment *n* is estimated using the adopted interface shear model:

$$\tau_n = f\left(u_{n(avg)}\right) \tag{6}$$

Step 5: Considering the force equilibrium in Segment *n*, unit tension at the front of this segment yields as follows:

$$T_{n-1} = T_n + 2.\Delta L.\tau_n \tag{7}$$

where ΔL = segment length. The average unit tension in Segment *n* ($T_{n(avg)}$) is then obtained:

$$T_{n(avg)} = \frac{T_n + T_{n-1}}{2} \tag{8}$$

Step 6: Tensile strain in Segment *n* is estimated using the adopted constitutive model for the geosynthetic and elongation of this segment (δ_n) is obtained:

$$\varepsilon_n = g^{-1}\left(T_{(avg)}\right) \tag{9}$$

$$\delta_n = \Delta L.\ \varepsilon_n \tag{10}$$

Step 7: Displacement at the front of Segment *n* is updated using u_n and δ_n:

$$u_{n-1} = u_n + \delta_n \tag{11}$$

The updated displacement at the front of Segment *n*, obtained in this step, is compared with that assumed in Step 3. If the difference between the two was negligible, proceed to the next step. Otherwise, the updated displacement is used in Step 3 and Steps 3 to 7 are iterated to converge.

Step 8: Steps 3–7 will be repeated for Segment *n-1* using the displacement and unit tension obtained at the end of this segment (u_{n-1} and T_{n-1}) to eventually determine the displacement and unit tension at the front of this segment. This procedure will then be repeated for Segments *n*-2 to 1 to obtain the displacement, strain, interface shear, and load profile along the geosynthetic length. Eventually, the geosynthetic frontal displacement (u_0) and frontal unit tension (T_0) will be determined.

Step 9: The incremental displacement in Step 1 is increased and the iteration is repeated to determine the updated load and displacement profiles along the geosynthetic.

Constitutive Models

The constitutive models adopted in this study to evaluate soil–geosynthetic interaction response in pullout tests are presented in this section.

Constitutive Model for Geosynthetic. The constitutive model adopted for the geosynthetic was consistent with the information typically provided by geosynthetic manufacturers. Specifically, the tensile loads correspond to 1, 2, 5, and 10% strains were identified and linear unit tension–strain relationships were considered between consecutive points.

Constitutive Model for Soil–Geosynthetic Interaction. Several interface shear models were evaluated in this study to simulate pullout test data. Ultimately, the two models finally adopted were those that could effectively explain the differences in the development of interface shear in various testing scales. Specifically, linear plastic and bilinear plastic soil–geosynthetic interface shear models were adopted, which are discussed in this section.

Linear Plastic Soil–Geosynthetic Interface Shear Model. A linear relationship between interface shear (τ) and geosynthetic

displacements (u) was defined using a slope referred to as the soil–geosynthetic shear stiffness (K_τ). The interface shear was limited by a maximum value referred to as the ultimate soil–geosynthetic interface shear (τ_{ult}) at a displacement value referred to as u_{ult}:

$$K_\tau = \frac{\tau_{ult}}{u_{ult}} \tag{12}$$

The ultimate soil–geosynthetic interface was estimated using the ultimate unit tension obtained in the pullout test (T_{ult}) and the confined contact area between soil and geosynthetic (2A):

$$\tau_{ult} = \frac{T_{ult}}{2A} \tag{13}$$

It should be noted that at the ultimate condition all geosynthetic segments displace at the same rate without developing significant additional strain. At this condition, a uniform interface shear was assumed along the geosynthetic.

The soil–geosynthetic shear stiffness (K_τ), or alternatively u_{ult}, was obtained after iterative procedure to minimize the sum of the squares of the residuals (S) between the experimental data and estimations made using the *t–z* analysis procedure adopted in this study.

Bilinear Plastic Soil–Geosynthetic Interface Shear Model. The linear plastic model was modified by splitting its linear portion into two linear portions using different soil–geosynthetic shear stiffness values. The stiffness adopted in the first linear portion was referred to as $K_{\tau-1}$ and that adopted in the second portion was $K_{\tau-2}$.

Two ratios were utilized to facilitate investigation of the optimum interface shear model. The displacement ratio (α) defines the ratio between the limit displacement value corresponds to the first linear portion of the model (u_1) and the displacement value corresponds to the ultimate interface shear (u_{ult}):

$$\alpha = \frac{u_1}{u_{ult}} \tag{14}$$

The interface shear ratio (β) defines the ratio between the limit interface shear corresponds to the first linear portion of the model (τ_1) and the ultimate interface shear (τ_{ult}):

$$\beta = \frac{\tau_1}{\tau_{ult}} \tag{15}$$

Scope of Experimental Program

A pullout testing program was conducted using three devices of different scales. Characteristics of the materials, specifications of the equipment, and the test procedure are described in this section.

Material Characteristics

Backfill Soil. The backfill material was Monterey No. 30 sand, which is a uniformly graded clean sand classified as SP (poorly graded). This sand has rounded to sub-rounded particles and consists predominantly of quartz with a trace of feldspars and other minerals. The grain size of Monterey No. 30 sand ranges from 0.2 to 2 mm with a mean grain size of 0.7 mm. The coefficients of uniformity and curvature are 1.9 and 1.3, respectively. The specific gravity of this soil is 2.65 and its minimum and maximum dry unit weight is14.76 and 16.70 kN/m^3, respectively. In this study, the backfill materials were placed at a moisture content of approximately 2% and were compacted using a hand tamper to reach a target dry unit weight of 16.05 kN/m^3.

Geosynthetic. The geosynthetic material was a polypropylene woven geotextile. This geotextile has mono-filament yarns oriented in the machine direction and multi-filament yarns oriented in the cross-machine direction. The unconfined tensile strength of this geosynthetic in the cross-machine direction, tested in this study, is 70 kN/m at failure and 19.3 and 39.4 kN/m at 2 and 5% strains, respectively.

Equipment and Test Setup

Pullout Test Device. Figure 2 shows a schematic layout of the testing devices. The devices were instrumented to map geosynthetic displacements in the confined and unconfined zones. The box dimensions (length × width × depth) were approximately 1,500 × 750 × 450 mm, 1,500 × 600 × 300 mm, and 250 × 300 × 150 mm for the large-, standard-, and small-scale devices, respectively. The confined length of geosynthetic specimens was approximately 1000, 600, and 250 mm and their width was approximately 750, 300, and 280 mm for the large-, standard-, and small-scale tests, respectively. A normal pressure of 21 kPa was generated on the geosynthetic specimens using two different systems. Roodi (*12*) extensively evaluated (and confirmed) consistency of the normal pressures generated by the two systems. In the large- and standard-scale setups, the normal pressure was applied using a set of six pneumatic actuators installed on top of a stack of wooden plates. The plates were backed with thick neoprene rubber mats to reduce the effect of rigidity. The pneumatic actuators were positioned to allow both piston extension and retraction to accommodate soil compression and dilation,

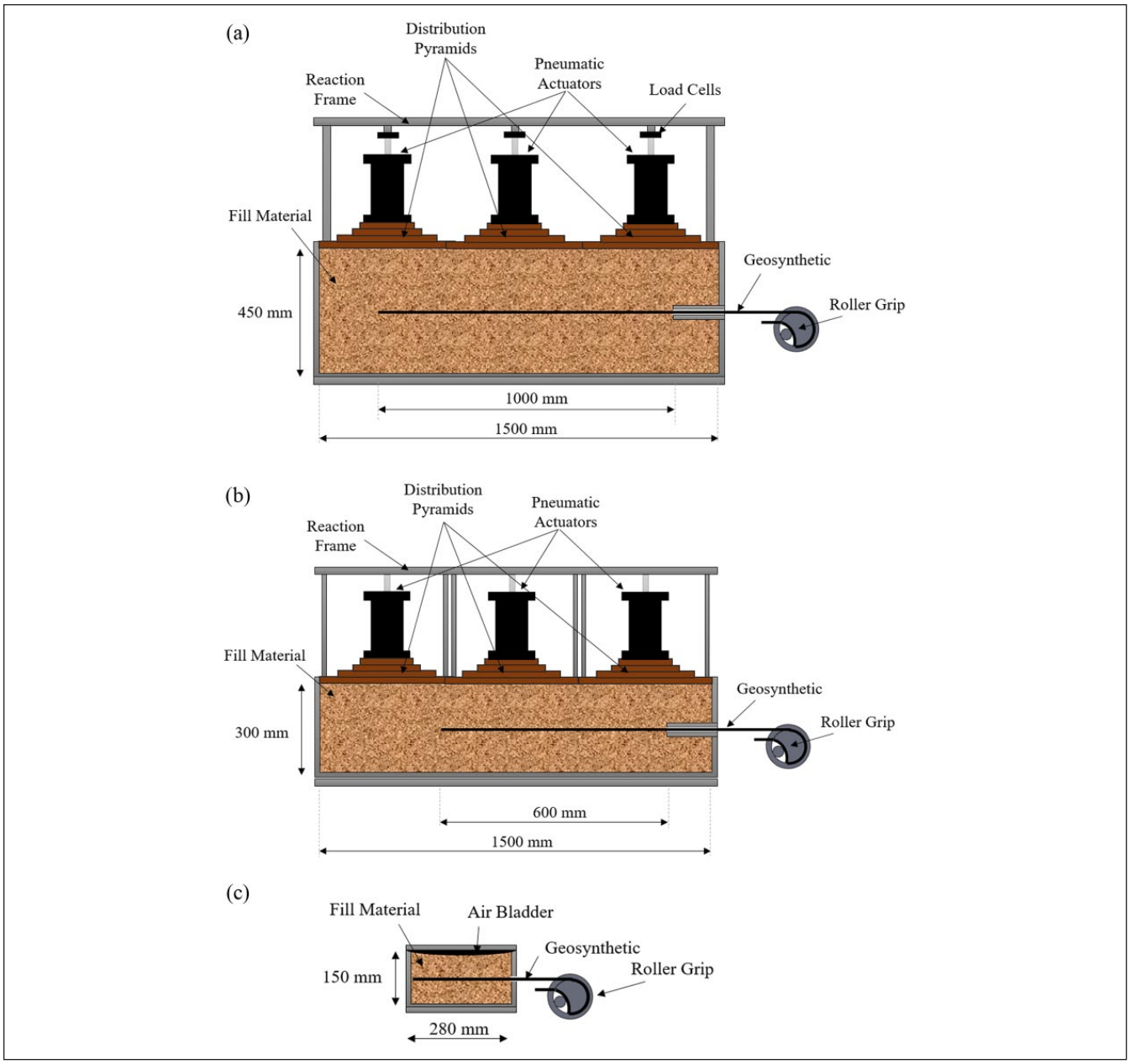

Figure 2. Schematics of pullout test equipment: (*a*) large-scale setup, (*b*) standard-scale setup, and (*c*) small-scale setup.

respectively. The load applied by the actuators was independently monitored during entire test using load cells. In the small-scale setup, the normal pressure was applied through an air bladder that was mounted in the box lid.

The geosynthetic was placed in the middle of the boxes and clamped to roller grips of different scales for the three different devices. The roller grips consisted of steel cylinders with crescent cuts. The clamp was lined with sandpaper to avoid geosynthetic slippage. The edge of the crescent cut in contact with the geosynthetic was lined with a neoprene foam strip to mitigate potential stress concentration at this location. This clamping system provides an unconfined geosynthetic section (i.e., outside the box), which allowed evaluation of the tensile behavior of the geosynthetic specimen during pullout tests. Pullout tests were conducted by pulling the grip at a rate of approximately 1 mm/min.

Results and Discussion

Experimental Test Results

The experimental data obtained from pullout tests conducted using the three scales of pullout devices are presented in Figure 3, *a–c*. The plots on the left presents the

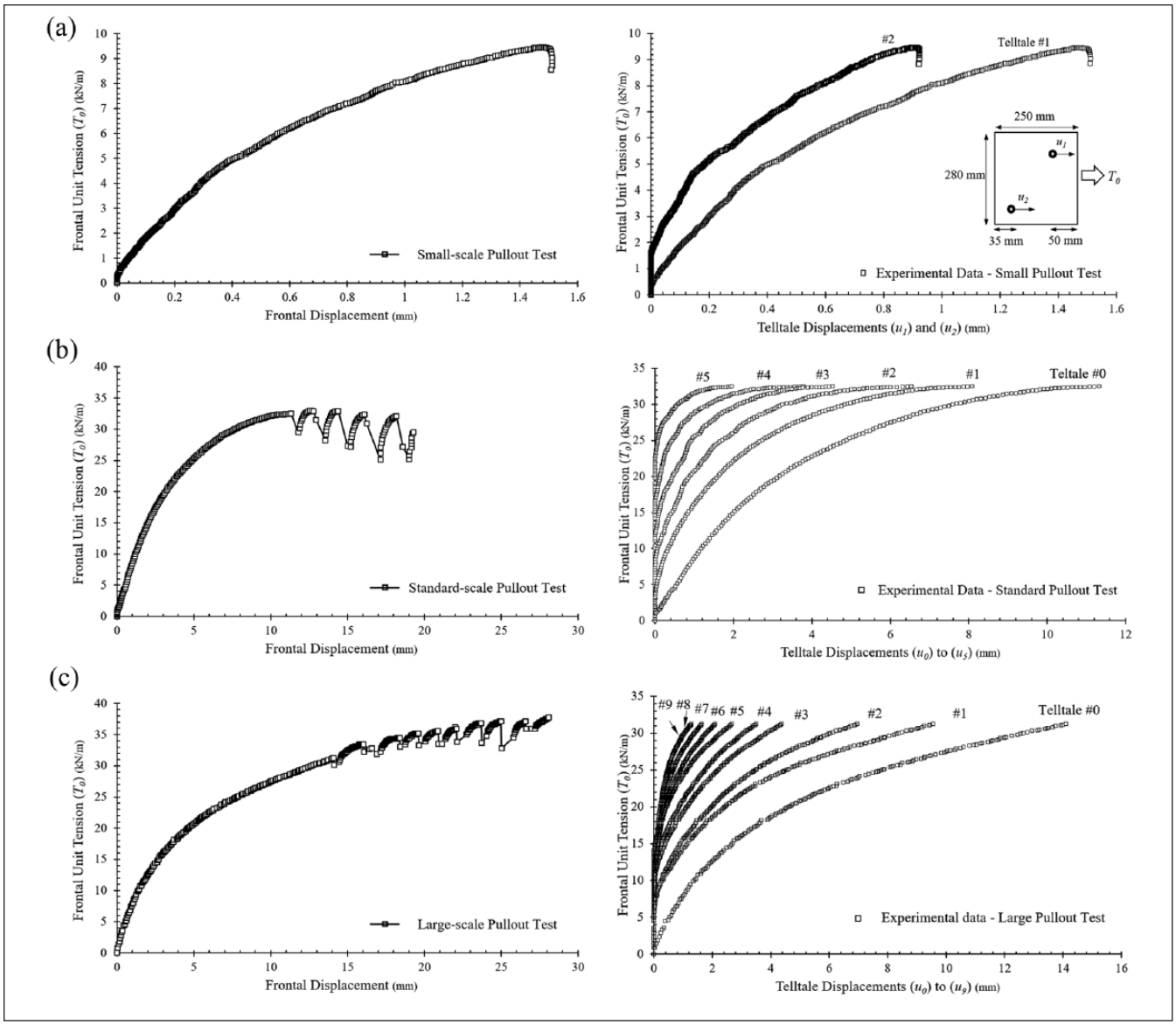

Figure 3. Frontal unit tension versus frontal displacements and versus geosynthetic displacements in the confined length: (*a*) small-scale test, (*b*) standard-scale test, and (*c*) large-scale test.

frontal unit tension versus frontal displacements and the plots on the right presents the frontal unit tension versus displacements along geosynthetic confined length recorded at telltale locations. Pullout tests stopped when (1) pullout load no longer increased and (2) displacement rate was the same along the geosynthetic. As shown in Figure 3, *b* and *c*, fluctuation in the unit tension was observed toward the end of the standard- and large-scale tests. This fluctuation, which was observed in the form of consecutive drops and recovery in the mobilized pullout resistance, is referred to as slip-stick mechanism in which temporary loss of resistance results from shear failure of soil adjacent to geosynthetic specimen. It should be noted that the plots on the right presents only the telltale data recorded before the slip-stick behavior starts.

The ultimate unit tension was found as approximately 10, 32, and 35 kN/m in the small-, standard-, and large-scale tests, respectively. Corresponding ultimate interface shear was calculated using contact areas between soil and geosynthetic in each test as 19.1, 26.0, and 18.6 kN/m^2, respectively. The slightly lower ultimate interface shear obtained in the small- and large-scale tests may be attributed to the comparatively higher coverage ratios (i.e., the ratio between geosynthetic confined area and the total soil area) and comparatively smaller clearance on the sides of the specimens to the sidewalls of the box in these scales as compared with the standard-scale test.

Understanding soil–geosynthetic interface shear response requires evaluation of the displacements recorded by telltales connected to the confined geosynthetic length. Specifically,

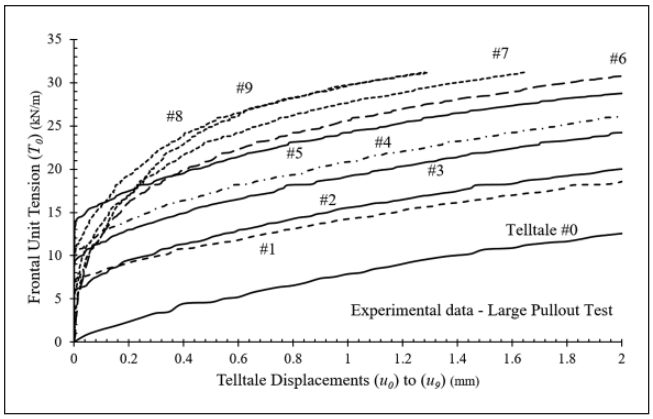

Figure 4. Close view of initial geosynthetic displacements in the confined length in the large-scale test.

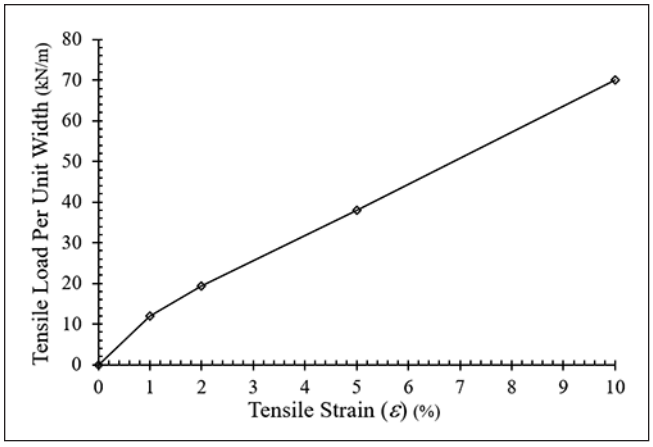

Figure 5. Geosynthetic constitutive model using data collected from geosynthetic unconfined length.

for evaluation of the data at small displacements, it is important to inspect the experimental data at the onset of the geosynthetic movement. Progressive mobilization of the interface shear resistance from pullout front toward the free end of the geosynthetic requires telltale displacements to be triggered in the order of their locations from the pulling front.

The displacement data recorded at the telltale locations versus frontal unit tension in the three pullout tests are also presented in Figure 3. As shown in Figure 3*a*, two telltales (Telltales #1 and #2) were installed in the small pullout test located 50 mm and 215 mm from the pulling front, respectively. The total number of telltales in the standard and large pullout tests was 6 and 10, respectively, out of which Telltale #0 was installed at the front of the confined geosynthetic length and the rest were equally spaced from the front to the free end of the geosynthetic. Inspection of the telltale data presented in Figure 3, *a* and *b*, indicates that the order of displacement triggering among various telltales was reasonably good in the small- and standard-scale tests. However, the data obtained from the large-scale test (Figure 3*c*) had to be studied carefully. Although telltales were attached to evenly spaced locations along the geosynthetic, it was found that Telltales #1 and #2 curves and Telltales #3 and #4 curves started at the same unit tension values.

A close view of the initial telltale displacements in the large-scale test is presented in Figure 4. Inspection of the data presented in this figure, reveals inconsistency in the expected order of triggered telltales and their movements thereafter. For example, although Telltales #6 to #9 were installed toward the free end of the geosynthetic, their displacements were triggered before those in Telltales #2 to #5. This inconsistency can be attributed to malfunction of the telltale attachments, waves in the geosynthetic, or effects from sidewalls and boundary conditions. Although this inconsistency might not be important in evaluation of pullout data at large displacements, it affects evaluations at small displacements. To minimize potential effects from misleading data, only the data represented by solid lines in Figure 4 were used in calibration of the interface shear model in this study. Displacements recorded at Telltales #1, #4, and #6 to #9 were discarded.

Geosynthetic Constitutive Model

Tensile characteristics of geosynthetic specimens were determined in each test using instrumentations installed in the unconfined portions of the geosynthetics. This information was compared with tensile characteristics reported by the geosynthetic manufacturer. Specifically, tensile loads corresponded to 1, 2, 5, and 10% strains were determined. As presented in Figure 5, the geosynthetic constitutive model was generated considering linear relationships between these data points. The difference between the tensile loads versus strain data obtained from the geosynthetics in the three testing scales was small. Therefore, the geosynthetic model presented in Figure 5 was used in simulation conducted for all testing scales.

Soil–Geosynthetic Constitutive Model

In this section, the *t–z* analysis procedure developed in this study was implemented to simulate the experimental data. Linear plastic and bilinear plastic models were used to find the optimum model for each scale. The ultimate interface shear values, calculated using the ultimate unit tensions, were used and model parameters were changed to obtain the best match to the experimental data. Specifically, u_{ult} was changed in the linear plastic interface model and $u_{ult}, u_1,$ and τ_1 (or alternatively, $u_{ult}, \alpha,$ and β) were changed in the bilinear plastic interface model. The model parameters corresponded to the lowest total sum of the squared residuals between measured and simulated displacements (for the same frontal unit tension) were determined.

Displacements recorded in the confined geosynthetic length at the telltale locations were used to find the soil–geosynthetic interface shear model in each testing scale. The displacements

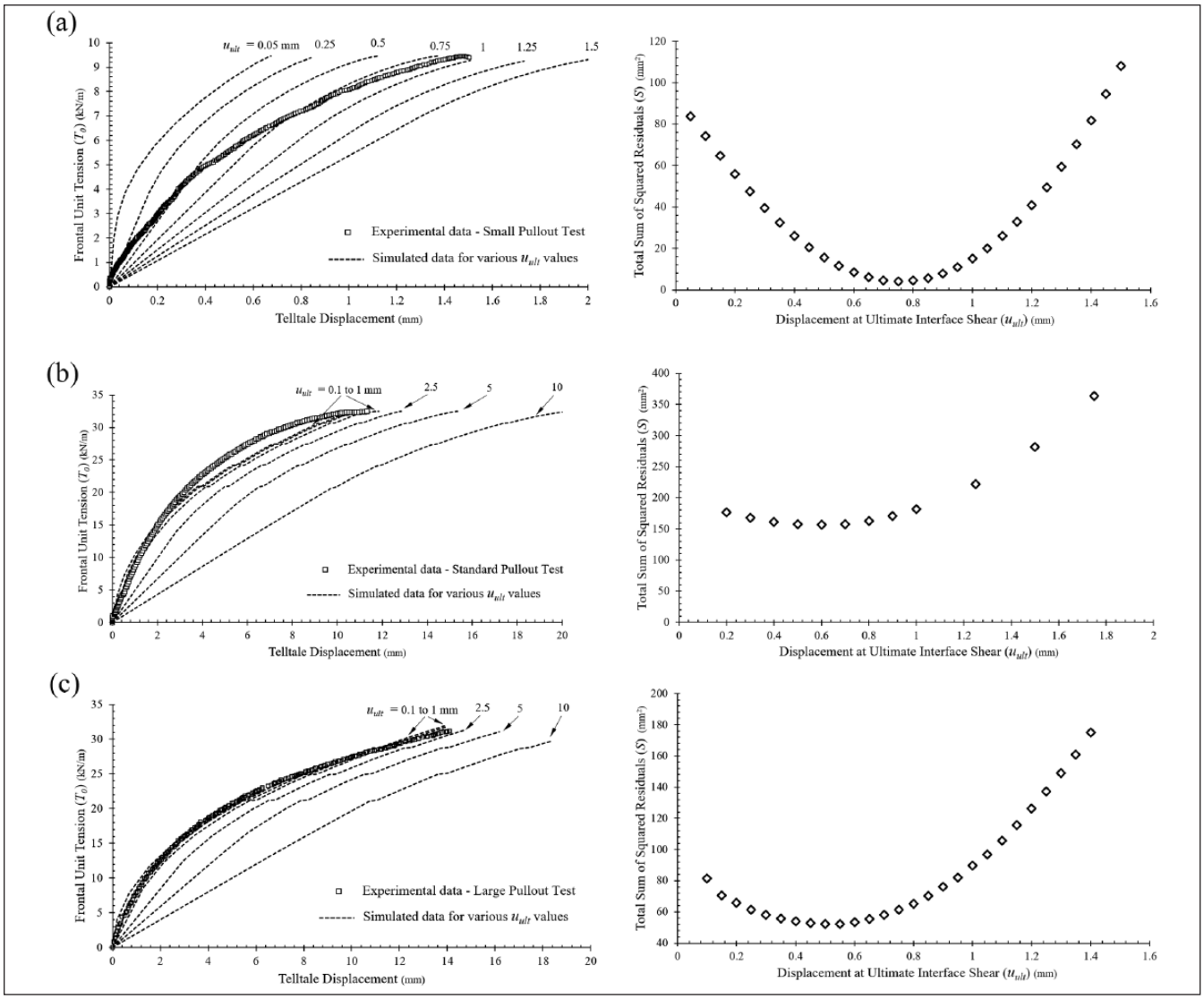

Figure 6. Simulation of the pullout test results using a linear plastic interface model and variation of the total sum of the squared residuals between the experimental and simulated data points: (*a*) small-scale test, (*b*) standard-scale test, and (*c*) large-scale test.

recorded at the end of the tests were used to estimate the displacement required to mobilize the ultimate soil–geosynthetic interface shear (u_{ult}). The ultimate pullout strength corresponds to the condition where the ultimate interface shear is mobilized over the entire interface area. At this condition, relative displacement between soil and geosynthetic is expected to exceed u_{ult} along the entire length of the geosynthetic. Therefore, the displacement recorded at the free end of the geosynthetic is expected to be a reasonably good estimate for u_{ult}. On the other hand, the displacement recorded at the pullout front corresponds to the displacement of the free end along with accumulated elongation of the entire geosynthetic.

Linear Plastic Interface Model. The limits of the displacement required to mobilize the ultimate interface shear, u_{ult}, was estimated using the experimental data presented in Figure 3. Specifically, u_{ult} was changed from 0.05 to 1.5 mm, from 0.1 to 10 mm, and from 0.1 to 10 mm to simulate the small-, standard-, and large-scale pullout test data, respectively. The *t–z* analysis was conducted using the algorithm previously detailed and the total sum of the squared residuals between the measured and simulated displacements (S) was determined. Figure 6 presents the simulated data as compared with the experimental data. Visual inspection of the data presented in this figure indicates that the linear plastic interface model could not reproduce the experimental data in the small-scale test (Figure 6*a*). However, the simulated data in the standard- and large-scale tests were found to be reasonably close to the experimental data for comparatively small values of u_{ult} (Figure 6, *b* and *c*).

Figure 6 also presents the total sum of the squared residual (S) between the experimental and the simulated data for various u_{ult} values. It should be noted that the S values in Figure 6 were computed considering the residual displacement values for all telltales. In the small-scale test, the lowest S value was

Table 1. Model Parameters and Total Sum of Squared Residuals Obtained in Simulations

Pullout Test Scale	Linear Plastic Interface Shear Model		Bilinear Plastic Interface Shear Model			
	u_{ult}	S	u_{ult}	α	β	S
Small pullout test	0.05	83.7	0.75	0.1	0.2	2.30
	0.25	47.4				
	0.5	15.6	1	0.2	0.5	0.79
	0.75	4.1				
	1	15.1	1.25	0.6	1	4.38
	1.25	49.6				
Standard pullout test	0.2	176.8	0.5	0.2	0.6	153.3
	0.5	157.4	0.6	0.1	0.5	147.3
	0.6	156.4	1.5	0.1	0.9	122.1
	1	181.9	2	0.1	0.9	122.2
	2.5	740.1	2.5	0.1	0.9	140.6
Large pullout test	0.1	81.5	0.5	1	1	52.3
	0.5	52.3	0.6	0.8	1	52.4
	0.6	53.5	0.75	0.7	1	52.4
	0.75	61.5	1.5	0.3	1	52.9
	1.5	204.0	2	0.3	1	53.8
	2	401.2	2.5	0.2	1	52.3

found to be 4.1 mm^2, which corresponded to u_{ult} = 0.75 mm. In the standard- and large-scale tests, the lowest *S* value was found to be 156.4 (corresponding to u_{ult} = 0.6 mm) and 52.3 mm^2 (corresponding to u_{ult} = 0.5 mm), respectively.

Bilinear Plastic Interface Model. A bilinear soil–geosynthetic interface shear model was also adopted to simulate the experimental pullout results. The simulation was aimed at refining the linear plastic model obtained in the previous section. Specifically, u_{ult} was changed from 0.75 to 1.25 mm, from 0.5 to 2.5 mm, and from 0.5 to 2.5 mm to simulate the small-, standard-, and large-scale test results, respectively. For each u_{ult} value, the displacement ratio (α) was changed from 0.1 to 1 by an increment of 0.1. The interface shear ratio (β) was then changed from α to 1 by an increment of 0.1. The optimum values for α and β were determined considering the lowest total sum of the squared residuals (*S*). It should be noted that interface shear ratios (β) lower than the displacement ratio (α) were not considered because the slope of the interface shear versus displacement relationship in the first linear portion of the bilinear model ($K_{\tau-1}$) was assumed to be always larger than this slope in the second linear portion of the model ($K_{\tau-2}$).

Table 1 summarizes the model parameters and resulting *S* values for the three testing scales and for both interface shear models. The *S* value in simulating the small-scale test results significantly decreased when a bilinear plastic model was used instead of a linear plastic model. The lowest *S* value in this testing scale was 0.79 mm^2, which corresponded to u_{ult} = 1 mm, α =0.2, and β =0.5.

Using the bilinear plastic model did not result in decreased values for *S* in simulating the large-scale pullout test. Specifically, the lowest *S* value obtained using the bilinear plastic model corresponded to cases where β =1 (or $\tau_1 = \tau_{ult}$), meaning that the stiffness of the second linear portion of the bilinear plastic model was zero ($K_{\tau-2} = 0$). In other words, the bilinear plastic models were equivalent of linear plastic models. Calculating $\alpha.u_{ult}$ for all bilinear plastic models for the large-scale test in Table 1 results approximately 0.5 mm. This is the same u_{ult} value as that corresponded to the lowest S value in this testing scale using a linear plastic model.

Evaluation of the results obtained for the standard-scale test in Table 1 indicates that the lowest value for *S* was obtained for a bilinear plastic model with u_{ult} =1.5 mm, α =0.1, and β = 0.9. The comparatively high value of β obtained in this case indicates that the stiffness of the second linear portion of the bilinear plastic model for the standard-scale test is comparatively small.

Relevant Interface Shear Model for Various Testing Scales. The interface shear models that resulted in the minimum *S* value for each testing scale and corresponding simulated telltale displacement data are presented in Figure 7. Comparison of the simulated and experimental data in Figure 7*a* indicates that using a bilinear plastic interface shear model was necessary to simulate telltale displacements in the small-scale pullout test. In contrast, the telltale displacements in the geosynthetic confined length in the large-scale pullout test could well be simulated using a linear plastic interface shear model (Figure 7*c*). Although the optimum model obtained to simulate the standard-scale pullout test data (Figure 7*b*) was bilinear plastic, this model was similar to an equivalent linear plastic model because the stiffness of the second linear portion was found to be very small.

Comparison of the slopes of the interface shear versus displacement relationships (and corresponding displacements) between the optimum models obtained for various testing scales underscores the different mechanisms involved in the development of interface shear. In the standard- and large-scale tests, the ultimate interface shear developed following a single slope (K_τ = 156 and 31 (kN/m^2)/mm, for the standard- and large-scale tests, respectively) at a geosynthetic displacement of 0.15 and 0.5 mm, respectively. On the other hand, in the small-scale test, half of the ultimate interface shear developed at comparatively smaller displacement of u_1 = 0.1 mm compared with that in the standard- and large-scale tests. However, additional shear resistance continued to develop up to a comparatively larger displacement of u_{ult} = 1 mm.

The comparatively high slope of the linear relationship between geosynthetic displacements and interface shear in the standard- and large-scale tests indicates that the ultimate interface shear at each point along the geosynthetic was fully mobilized at comparatively small displacements.

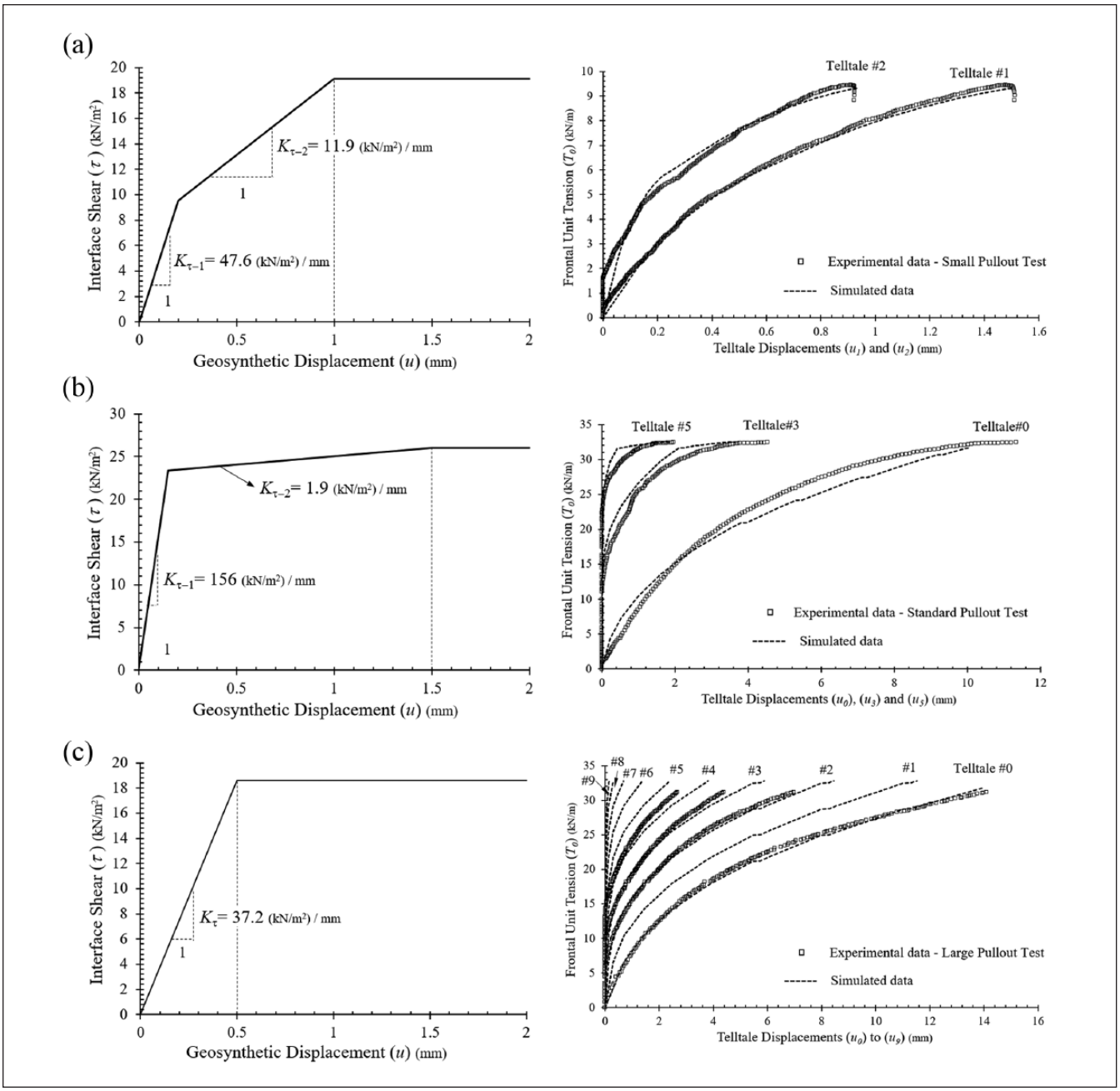

Figure 7. Optimum interface shear model obtained for various testing scales and experimental data versus simulation results using the obtained optimum interface shear model: (*a*) small-scale test, (*b*) standard-scale test, and (*c*) large-scale test.

Therefore, additional displacements would not necessarily increase the pullout resistance. Instead, additional pullout resistance was developed as the mobilized length of the geosynthetic increased. Consequently, the ultimate pullout resistance was reached shortly after the entire length of the geosynthetic was mobilized. In contrast, in the small-scale test, shear resistance was mainly developed by increased displacements. Consequently, unlike the larger scale tests, in the small-scale test significant additional resistance was developed even after the entire length of the geosynthetic was mobilized.

Displacements, Strains, and Interface Shear along Geosynthetics

The geosynthetic displacements measured in the confined portion of the geosynthetics were compared with the simulated data obtained for each testing scale. The simulated displacements are presented for the optimum models obtained for each scale at various levels of frontal unit tension. In addition, variation of the tensile strain in the geosynthetic confined portion and the interface shear values estimated along geosynthetics are also discussed.

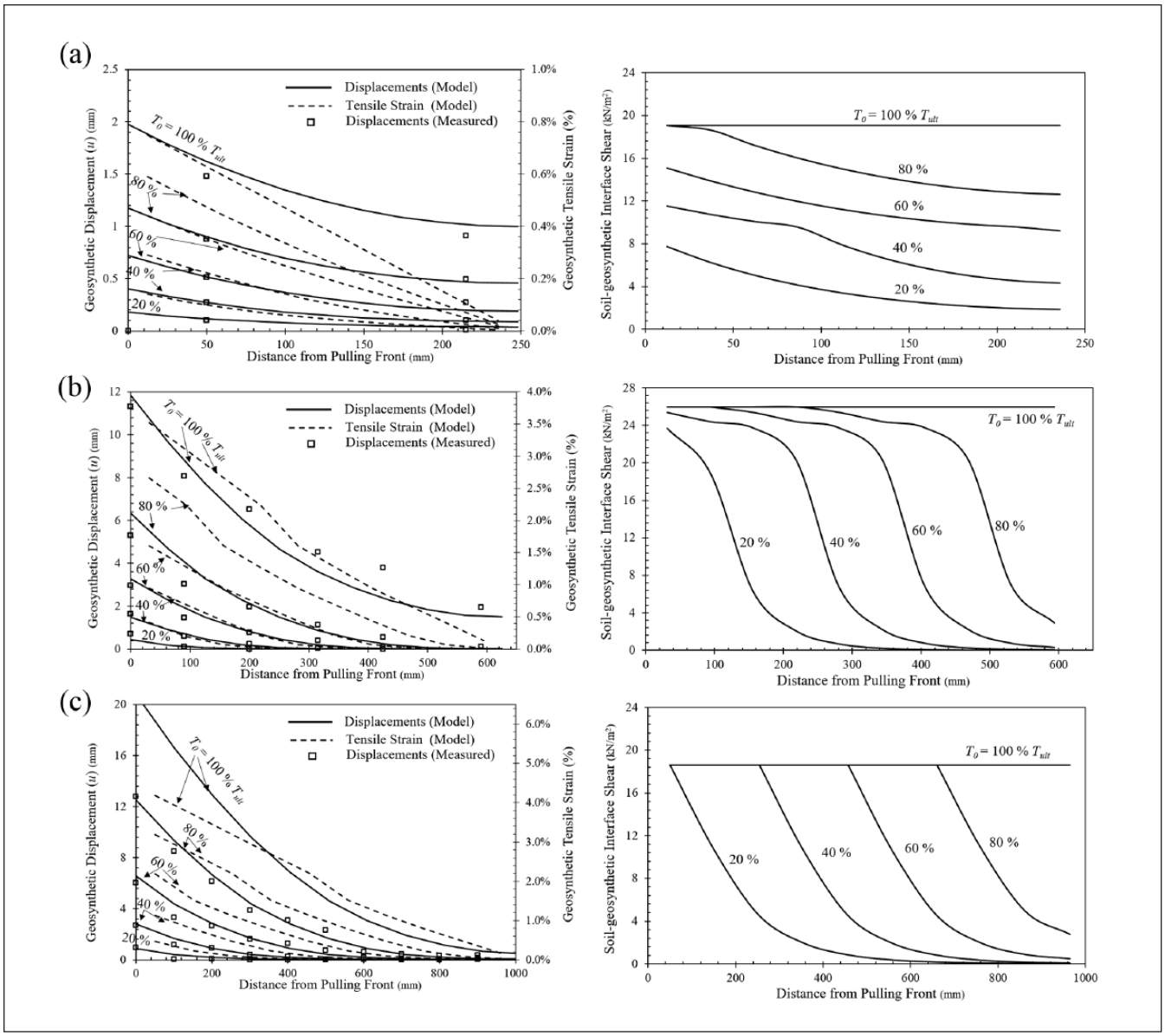

Figure 8. Displacements, tensile strains, and soil–geosynthetic interface shear along geosynthetics at various levels of ultimate frontal unit tension: (*a*) small-scale test, (*b*) standard-scale test, and (*c*) large-scale test.

Figure 8 presents displacements, tensile strains, and interface shear estimated along the geosynthetics at 20, 40, 60, 80, and 100% of the ultimate frontal unit tension. Comparison of the measured displacements with simulated displacements underlines suitability of the models obtained in various testing scales. In addition, comparison between the mobilized lengths of the geosynthetics at various levels of frontal unit tension further underscores the different interface shear mobilizations among the testing scales. In the small-scale test, the total length of the geosynthetic mobilized at a comparatively low frontal unit tension (20%) and the entire geosynthetic displaces thereafter. This condition was not interpreted as the ultimate pullout condition because the specimen continued to mobilize additional pullout resistance and the displacement rate was also not the same along the geosynthetic. However, as a result of the movement of the entire specimen, comparatively small tensile strains (elongations) developed in the geosynthetic in this testing scale. In the standard- and large-scale pullout tests, however, the active length of the geosynthetic continued to increase as the interface shear resistance progressively mobilized. The ultimate frontal unit tension was reached shortly after shear was mobilized along the entire length of the geosynthetic. Therefore, comparatively large deformations (elongations) developed in the geosynthetic in these testing scales.

In the standard- and large-scale tests, the interface shear was found to be distributed differently over three sections along the geosynthetic. The interface shear was found to be

comparatively uniform in the frontal portion (i.e., toward the pullout front) of the geosynthetic. Then, along a transition section, the interface shear reduces to approximately zero in the stationary length of the geosynthetic (i.e., toward the free end; Figure 8, *b* and *c*). In the small-scale test, however, the interface shear was found to have a continuous profile along the entire geosynthetic length (Figure 8*a*). The shape of this profile was found to change as the frontal unit tension increased. At comparatively large displacements, the interface shear was found to be uniformly distributed over the portion of the length within which displacements exceeded u_{ult}. The interface shear gradually reduced in the remaining length of the geosynthetic within which displacements were below u_{ult}.

Summary and Conclusions

The development of soil–geosynthetic interface shear was studied using experimental data obtained from pullout tests conducted on a woven geotextile in a uniformly graded sand under a normal pressure of 21 kPa at three different testing scales. Unlike conventional analytical approaches in evaluation of pullout test results in which constitutive models for soil–geosynthetic interface shear and geosynthetic material were typically determined using additional tests (e.g., direct shear test, wide width tensile test), this study adopted a procedure in which the pullout test results can directly be used to identify constitutive models for the soil–geosynthetic interface shear and the geosynthetic. Specifically, the constitutive model for geosynthetic specimen was estimated from data collected in the unconfined portion of the geosynthetic. The soil–geosynthetic interface shear model was obtained by simulating the displacements measured in the geosynthetic confined length. The procedure adopted for this simulation was similar to the *t–z* analysis procedure originally developed to simulate piles subjected to axial loading. As part of this study, several interface shear models were evaluated. The two models that were eventually adopted were those that could underscore the difference in the development of interface shear in various testing scales. Specifically, linear plastic and bilinear plastic soil–geosynthetic interface shear models were adopted.

Comparison of the experimental and simulated data for the standard- and large-scale tests revealed that a linear plastic model can adequately define the soil–geosynthetic interface shear responses in these scales. The slope of the linear relationship between interface shear and geosynthetic displacements was found to be comparatively high. Consequently, in the standard- and large-scale tests, the ultimate interface shear at each point along the geosynthetic developed at comparatively small displacements. Therefore, the development of additional interface shear resistance required increased geosynthetic active length. Progressive mobilization of the interface shear continued until shear was mobilized along the entire length of the geosynthetic.

The development of soil–geosynthetic interface shear in the small-scale test was found to differ from that obtained for the standard- and large-scale tests. Specifically, a bilinear plastic model was found to be necessary to define the soil–geosynthetic interface shear response in the small-scale test. The slope of the interface shear versus geosynthetic displacement at the onset of the movement was found to be particularly high. This means that significant interface shear primarily mobilizes at comparatively small geosynthetic displacements. However, the slope of the second linear portion of the bilinear interface shear model was found to be smaller than the first portion. This means that after initial mobilization of shear, the development of additional shear resistance required comparatively larger displacements. Consequently, in the small-scale test, significant additional shear resistance was found to develop even after shear was mobilized along the entire length of the geosynthetic.

As comparatively small elongation was found in the geosynthetic in the small-scale test, the interface shear resistance in this scale developed mainly by displacement of the entire geosynthetic. In the standard- and large-scale tests, however, the entire geosynthetic did not significantly displace. Instead, the interface shear resistance in these scales developed mainly by deformation (elongation) of the geosynthetic.

Findings from this study suggest that the differences among pullout test results obtained using different test scales may partially be attributed to differences in mobilization of the interface shear resistance. Gaining better understanding of the impact of testing scale on soil–geosynthetic interaction data may be particularly important in adopting each testing scale for appropriate applications. Although a large-scale device may be essential for characterization of ultimate conditions, a small-scale test may be appropriate to be used for working conditions and small-displacement responses. Specifically, using a small-scale test device maybe relevant for specification of a soil–geosynthetic composite property under small displacements, which is particularly relevant for practical applications, such as the base stabilization of roadways.

References

1. Brown, S. F., J. M. Brunton, D. A. B. Hughes, and B. V. Brodrick. Polymer Grid Reinforcement of Asphalt. *Asphalt Paving Technology*, Vol. 54, 1985, pp. 18–41.
2. Al-Qadi, I. L., S. H. Dessouky, J. Kwon, and E. Tutumluer. Geogrid in Flexible Pavements: Validated Mechanism. *Transportation Research Record: Journal of the Transportation Research Record*, 2008. 2045: 102–109.
3. Zornberg, J. G., G. H. Roodi, J. Ferreira, and R. Gupta. Monitoring Performance of Geosynthetic-Reinforced and Lime-Treated Low-Volume Roads Under Traffic Loading and

Environmental Conditions. *Proc., GeoCongress 2012: State of the Art and Practice in Geotechnical Engineering*, Oakland, Calif, ASCE, Reston, VA, 2012, pp. 1310–1319.
4. Bathurst, R. J., T. M. Allen, and D. L. Walters. Reinforcement Loads in Geosynthetic Walls and the Case for a New Working Stress Design Method. *Geotextiles and Geomembranes*, Vol. 23, No. 4, 2005, pp. 287–322.
5. Morsy, A. M., J. G. Zornberg, B. R. Christopher, D. Leshchinsky, B. F. Tanyu, and J. Han. Experimental Approach to Characterize Soil-Reinforcement Composite Interaction. *Proc., 19th ICSMGE*, Seoul, Korea, ISSMGE Open Access Online Library, London, UK, 2017, pp. 451-454.
6. Chen, Q., and M. Abu-Farsakh. Structural Contribution of Geogrid Reinforcement in Pavement. *Proc., GeoCongress 2012: State of the Art and Practice in Geotechnical Engineering*, Oakland, California, ASCE, Reston, Va., 2012, pp. 1468–1475.
7. Weldu, M. T., J. Han, S. M. Rahmaninezhad, R. L. Parsons, J. I. Kakrasul, and Y. Jiang. Effect of Aggregate Uniformity on Pullout Resistance of Steel Strip Reinforcement. *Transportation Research Record: Journal of the Transportation Research Record*, 2016. 2579: 1–7.
8. Morsy, A. M., D. Leshchinsky, and J. G. Zornberg. Effect of Reinforcement Spacing on the Behavior of Geosynthetic-Reinforced Soil. *Proc., Geotechnical Frontiers*, Orlando, Forida, ASCE, Reston, VA, USA 2017, pp. 112–125.
9. Roodi, G. H., and J. G. Zornberg. Stiffness of Soil-Geosynthetic Composite under Small Displacements: II. Experimental Evaluation. *Journal of Geotechnical and Geoenvironmental Engineering*, Vol. 143, No. 10, 2017, p. 04017076.
10. Zornberg, J. G., G. H. Roodi, and R. Gupta. Stiffness of Soil-Geosynthetic Composite under Small Displacements: I. Model Development. *Journal of Geotechnical and Geoenvironmental Engineering*, Vol. 143, No. 10, 2017, p. 04017075.
11. Juran, I., and C. L. Chen. Soil-Geotextile Pull-Out Interaction Properties: Testing and Interpretation. *Transportation Research Record*: *Journal of the Transportation Research Record*, 1988. 1188: 37–47.
12. Roodi, G. H. *Analytical, Experimental, and Field Evaluations of Soil-Geosynthetic Interaction under Small Displacements*. PhD dissertation. University of Texas, Austin, 2016.
13. Yuan, Z. Pullout Response of Geosynthetic in Soil-Theoretical Analysis. *Proc., Geo-Frontiers 2011: Advances in Geotechnical Engineering*, Dallas, Tex., ASCE, Reston, VA, USA 2011, pp. 4388–4397.
14. Bergado, D. T., and J. C. Chai. Pullout Force–Displacement Relationship of Extensible Grid Reinforcements. *Geotextiles and Geomembranes*, Vol. 13, No. 5, 1994, pp. 295–316.
15. Wilson-Fahmy, R. F., and R. M. Koerner. Finite Element Modeling of Soil-Geogrid Interaction with Application to the Behavior of Geogrids in a Pullout Loading Condition. *Geotextiles and Geomembranes*, Vol. 12, No. 5, 1993, pp. 479–501.
16. Perkins, S. W., and E. V. Cuelho. Soil-Geosynthetic Interface Strength and Stiffness Relationships from Pullout Tests. *Geosynthetics International*, Vol. 6, No. 5, 1999, pp. 321–346.
17. Farrag, K., A. B. Yalcin, and I. Juran. Pull-Out Resistance of Geogrid Reinforcements. *Geotextiles and Geomembranes*, Vol. 12, 1993, pp. 133–159.
18. Moraci, N., and P. Recalcati. Factors Affecting the Pullout Behaviour of Extruded Geogrids Embedded in a Compacted Granular Soil. *Geotextiles and Geomembranes*, Vol. 24, No. 4, 2006, pp. 220–242.
19. Palmeira, E. M. Soil–Geosynthetic Interaction: Modelling and Analysis. *Geotextiles and Geomembranes*, Vol. 27, No. 5, 2009, pp. 368–390.
20. Chin, J. T., and H. G. Poulos. A "T-Z" Approach for Cyclic Loading Analysis of Single Piles. *Computers and Geotechnics*, Vol. 12, 1991, pp. 289–320.
21. Coyle, H. M., and I. H. Sulaiman. Skin Friction for Steel Piles in Sand. *Soil Mechanics and Foundation*, Vol. 93, No. SM6, 1967, pp. 261–278.
22. Vijayvergiya, V. N. Load-Movement Characteristics of Piles. *Proc. Ports '77, 4th Annual Symposium of the American Society of Civil Engineers*, Waterway, Port, Coastal and Ocean Division, Long Beach, CA, 1977, pp. 269–284.
23. McVay, M. C., F. C. Townsend, D. G. Bloomquist, M. O. O'Brien, and J. A. Caliendo. Numerical Analysis of Vertically Loaded Pile Groups. *Proc., Foundation Engineering: Current Principles and Practices*, Evanston, Illinois, ASCE, Reston, VA, 1989, pp.675–690.
24. Randolph, M. F. Design Methods for Pile Groups and Piled Rafts. *Proc., 13th ICSMFE*, New Delhi, Oxford and IBH Publishing Co. Pvt. Ltd., New Delhi, India, Vol. 5, 1994, pp. 61–82.
25. Beech, J.F. Importance of Stress-Strain Relationships in Reinforced Soil System Design. Proc., Geosynthetic '87, New Orleans, Louisiana, Industrial Fabrics Association Int., St Paul, MN, 1987, pp. 133-144.
26. Teixeira, S.H.C., B.S. Bueno, and J.G. Zornberg. Pullout Resistance of Individual Longitudinal and Transverse Geogrid Ribs. *Journal of Geotechnical and Geoenvironmental Engineering*, Vol. 133, No. 1, 2007, pp. 37-50.

The Standing Committee on Geosynthetics (AFS70) peer-reviewed this paper (18-06179).